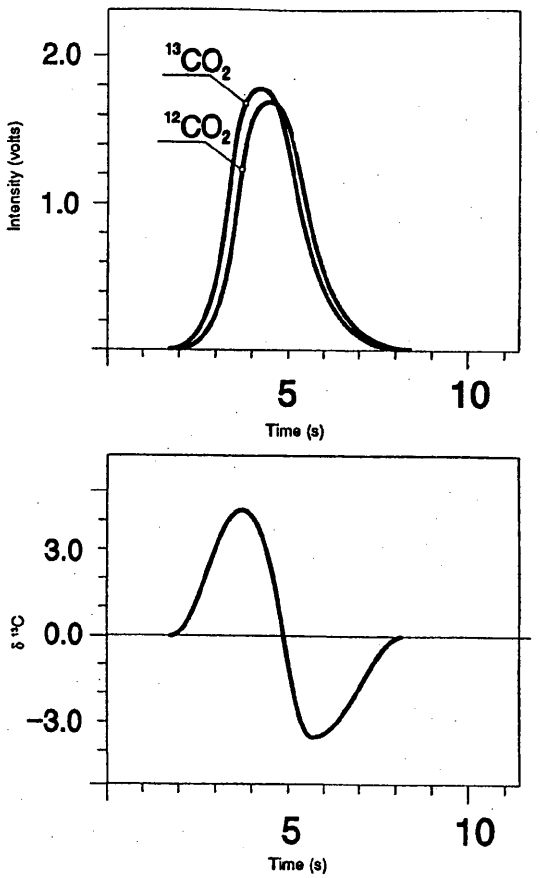

Fig. 2. Illustration of the time displacement between $^{13}CO_2$ and $^{12}CO_2$ that causes the S-shaped 45/44 ratio signal [5]. From Ref. [5], ©Intercept 1990.

from the column because of its higher vapour pressure and, hence, lower boiling point as compared to the heavier isotope species.

Although baseline separated peaks should be the ultimate goal in GC–C–IRMS, there is many an application where overlapping peaks simply cannot be avoided. In addition, CO_2 and N_2 disperse more freely within the carrier gas stream than their parent organic compounds resulting in overlapping CO_2 peaks for barely baseline resolved GC peaks. To extract the valuable information obscured by such peak overlaps, Goodman and Brenna [13,14] suggested software algorithms for improved data processing. These algorithms were based on curve fitting rather than the summation (the industrial standard) using combinations of exponentially modified Gaussian (*E*) and Harhoff/Van-der-Linde (*H*) functions and were tested on up to 70% valley peak overlap. When the adjacent peaks were of equal abundance (leading peak:trailing peak, 1:1) combinations of HE and HH appeared to provide the best recovery of isotope ratios. In the case of unequal abundance in favour of the leading peak (10:1), the HH combination gave the best accuracy. When the abundance was reversed (1:10), the EH combination provided the best accuracy but only for peak overlap up to 40% valley. Despite these encouraging results, curve-fitting algorithms for restoring lost accuracy have not been incorporated into any commercial IRMS data reduction software by IRMS manufacturers. It could be argued that the potential of curve-fitting algorithms was only demonstrated on two compounds, methyl tridecanoate and butylated hydroxytoluene, which were of almost identical carbon isotope ratios and that any curve-fitting software should also be able to extract accurate and precise isotope ratios of two overlapping compound peaks with different carbon isotope ratios. However, any progress in this direction needs to be aided by full evaluation of new algorithms for routine use (under 'real life conditions'), thus requiring wide user access to such algorithms which in turn depends on the support from IRMS manufacturers.

2.2.1. Sample preparation

To achieve high-precision CSIA by GC–C–IRMS the following points must be considered:

(1) Every step of the sample preparation protocol (collection, work up, derivatization) must be scrutinised for potential mass discriminatory effects to avoid isotopic fractionation of the target compounds.

(2) If the potential of isotopic fractionation cannot be ruled out conclusively, an internal standard, of a similar chemical nature (but not requiring derivatization) and of known isotopic composition, should be added to the sample prior to sample preparation.

(3) Signal size and isotopic composition of the standard(s) must match those of the analyte(s) [15].

(4) The potential of all GC parameters (polarity of stationary phase, carrier gas management, temperature programme) and techniques should be exploited to their fullest to achieve HRcGC.

2.2.1.1. Derivatization

Despite their importance for high-precision CSIA, dedicated studies addressing issues of sample preparation are few and far between. Schumacher et al. compared different sample preparation methods for isotopic analysis of volatile organic compounds (VOCs) from strawberries [16]. Khalfallah et al. reported a correction method to compensate for ^{13}C tracer dilution by carbon added during derivatization [17], and a carbon balance equation was described by Demmelmair and Schmidt to calculate $\delta^{13}C$ values of free amino acids from $\delta^{13}C$ values of their derivatives at natural abundance level [18]. Kinetic isotope effects associated with derivatization reactions and resulting theoretical considerations for calculating $\delta^{13}C$ values have been discussed by Rieley [19].

Of course, one way of avoiding the problems with derivatization is not to derivatize the sample at all. This approach involves the use of moderately polar to polar stationary phases and high-temperature GC. However, not all polar compounds are amenable to these techniques (e.g., amino acids) and high-temperature capability of polar stationary phases is limited even when oxygen free helium is used as carrier gas.

In addition to changes in ^{13}C isotopic signature by derivatization, its effects on GC separation and sample conversion into CO_2 and N_2 have to be considered. Derivatization by silylation might hamper GC separation as the apolar nature of trimethylsilyl (TMS) and *tert.*-butyldimethylsilyl (*t*BDMS) derivatives can obscure compound characteristics that could otherwise be chromatographically exploited. Furthermore, an excessive carbon load introduced by derivatization might result in incomplete combustion thus compromising accurate isotopic analysis. For reasons of non-quantitative sample conversion, the use of trifluoroacetates (TFA) or heptafluorobutyrates (HFB) is not advisable as fluorine forms extremely stable fluorides with Cu and Ni, thus irreversibly reducing combustion efficacy of the CuO/NiO system. In addition, fluorine poisons the combustion catalyst platinum. Experiments with *N*-TFA, *O*-propylates of alanine and leucine have shown that only 50% of the expected CO_2 yield was produced [20].

2.2.2. Isotopic calibration

For reasons mentioned before, it is not possible in GC–C–IRMS to calibrate target compounds against a standard of known isotopic composition, introducing the standard in exactly the same way as the analyte. There are only three feasible means of introducing a standard: (a) addition of reference compounds to the sample, (b) introduction of reference gas pulses to the carrier gas stream, or (c) introduction of reference gas pulses directly into the ion source.

Caimi et al. comprehensively listed all the desirable properties internal reference compounds should possess: (1) high chemical stability; (2) conveniently available in high purity; (3) readily soluble in high-purity solvents; (4) low vapour pressure at room temperature and atmospheric pressure; (5) environmentally rare; (6) ideally useful for GC and liquid chromatography (LC) techniques; and (7) sufficiently different chromatographic characteristics to avoid partial or complete co-elution with sample analytes [21].

The results of an extensive study into methods of isotopic calibration by Merritt et al. emphasised these demands [22]. Comparing the use of internal reference compounds with the introduction of reference gas pulses directly in the ion source of the IRMS, Merritt et al. found an offset of >2‰ between the two methods in the case of incomplete combustion and other systematic errors affecting only the analytes. These systematic errors affected both the analytes and the co-injected reference compounds but were not reflected by the external reference gas pulses. Similar observations were made by other groups interested in isotopic calibration [12,21,23]. In the absence of such systematic errors, Merritt et al. found that both methods of isotopic calibration gave consistent results as long as multiple reference peaks were used to permit drift correction. Only one reference peak for isotopic calibration, albeit from an internal reference compound, is not enough to compensate for the influence of GC parameters, such as analyte/stationary phase interaction, column temperature on measured isotope ratios [12].

Within the GC–C–IRMS system, seven potential sources for mass discrimination and, hence, sys-

tematic errors can be identified: (1) isotopic fractionation during sample injection (which can be overcome by on-column or time programmed splitless injection); (2) chromatographic isotope effect; (3) chromatographic peak distortion (leading and trailing peak tail); (4) combustion process; (5) peak distortion of N_2/CO_2 gas peak during passage of the combustion interface; (6) changing flow conditions at the open split prior to the IRMS; and (7) the IRMS itself. Obviously, the external reference gas pulses only compensate for item (7), whereas internal reference compounds reflect all of the aforementioned. Recently, a method for isotopic calibration was reported that, provided a combustible gas was used, could reflect the systematic errors caused by items (4–7) [24]. This method combines the convenience and practicability of external reference gas calibration with the advantage of reflecting the majority of physical influences to which analytes are subjected in a GC–C–IRMS system.

2.2.3. HRcGC

As pointed out earlier, baseline separated gas chromatographic peaks are the basis for high-precision CSIA. To achieve this goal, in the first instance, basic gas chromatographic rules must be observed: (1) the polarity of the stationary phase should meet the polarity of the analytes; (2) column head pressure and, hence, carrier gas velocity, should be set to suit column diameter; and (3) temperature gradients should be chosen to exploit the maximum of the column length (the longer the column, the slower the temperature rise per minute; cf. Table 1) [25].

Further to these principles, HRcGC techniques such as multi-dimensional capillary GC (MDcGC), enantio-selective GC, porous layer open tubular (PLOT) column GC for analysis of VOCs and high-temperature capillary GC (HTcGC) are powerful tools for high-precision CSIA when used in combination with GC–C–IRMS. Nitz et al. were the first to report the advantages of using MDcGC in GC–C–IRMS [26]. MDcGC is now, often in combination with enantioselective GC, almost exclusively used in authenticity control of flavours and fragrances by CSIA [27,28]. In a similar fashion, HTcGC is strongly associated with CSIA of steroids and long-chain fatty acids (e.g., Ref. [29]).

Regrettably, the achievements of HRcGC in terms of well-defined peak shape and baseline separation are likely to be impaired during combustion and the subsequent passage through the interface. Changes in tubing diameter and frequent use of unions to connect the various parts of tubing lead to a loss in peak definition (peak broadening; peak distortion) and even to partial peak overlap, all of which have a detrimental effect on accuracy and precision of isotope ratio measurement [12]. Very recently, Goodman reported a single-capillary interface design (SCID) which he developed to overcome these problems [30]. As the name suggests, a single capillary was used to connect the GC column to the open-split in front of the IRMS. This capillary was threaded through a furnace and accommodated two

Table 1
Recommended values for carrier gas velocity and temperature gradient according to column length when using helium as carrier gas[a]

Column length (m)	Elution of methane (s)[b]	Temperature gradient (°C/min)
10	35	2.5
15	53	1.65
20	70	1.25
25	88	1.05
30	105	0.84
40	140	0.63
50	175	0.5

[a]Based on working directions given by Grob [25].
[b]Set GC oven temperature to 30°C. Set split ratio to about 1:30, inject a few μl of natural gas (or lighter gas) and measure elution time of the first peak (FID signal). Adjust column head pressure to match recommended elution time.

CuO wires positioned thus as to coincide with the furnace dimensions. So far, this design has been tested for ^{13}C isotopic abundance analysis of *n*-alkanes.

3. High-precision CSIA of ^{13}C isotopic abundance

3.1. GC–C–IRMS at natural abundance level

High-precision CSIA of ^{13}C isotopic abundance at both natural abundance (NA) and low enrichment level can yield measurements of $\delta^{13}C$ values with a precision of 0.3‰ on average. Thanks to this high precision, even small changes in ^{13}C isotopic abundance of 1‰ can be reliably detected. For this reason GC–C–IRMS has become the method of choice to determine the origin of a given organic compound by measuring its characteristic isotope 'finger print'.

In contrast to the generally held opinion, the natural abundance of stable isotopes is not a fixed constant but displays a considerable, yet subtle, degree of variation. The variation on the natural abundance of ^{13}C can be as high as 0.1 at.% (Fig. 3). This wide range reflects the varying degree of mass

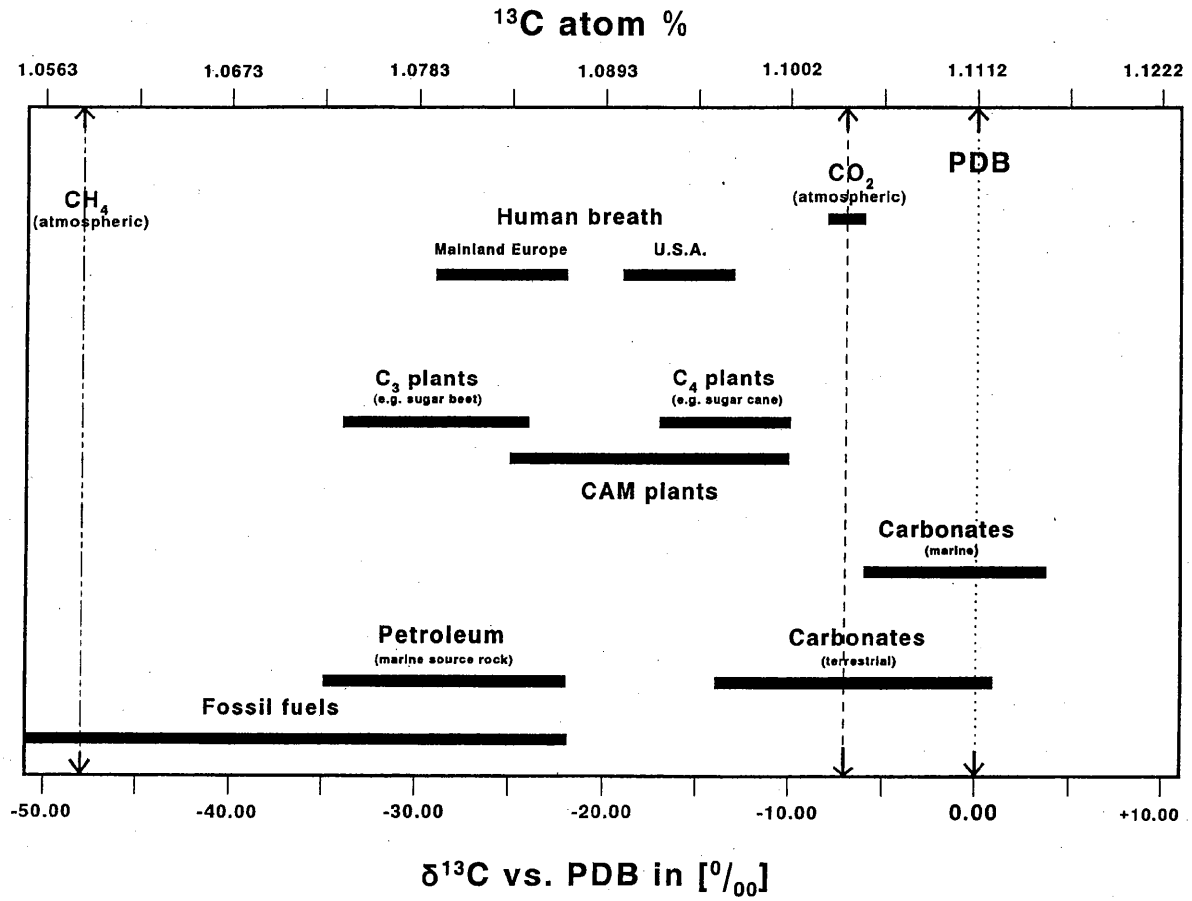

Fig. 3. Some typical examples of natural $\delta^{13}C$ values grouped according to origin along the scale of ^{13}C natural abundance.

discrimination associated with the different pathways of carbon assimilation and fixation. To give an example, in terms of ^{13}C isotopic abundance, beet sugar is not the same as cane sugar. In sugar beet CO_2 fixation results in the formation of a C_3 body, 3-phosphoglycerate (3-PGA). This pathway of CO_2 fixation is known as the Calvin cycle. Plants using the 3-PGA pathway for CO_2 fixation are commonly called C_3 plants. However, some plants, of which sugar cane is one, make use of a different pathway. Here, CO_2 fixation yields a C_4-dicarboxylic acid, oxalo acetate, hence the term C_4 plants (the C_4-dicarboxylic acid pathway is also known as the Hatch–Slack cycle). The products of these two pathways are characterised by their different ^{13}C abundance. Glucose derived from C_3 plants has a $\delta^{13}C$ value of about −25‰, whereas glucose derived from C_4 plants exhibits a more positive $\delta^{13}C$ value of about −11‰ indicating a mass discriminatory bias towards $^{13}CO_2$ of the Hatch–Slack cycle.

Differences in $\delta^{13}C$ values were reported for total leaf tissue, total surface lipid extracts, and individual *n*-alkanes isolated from plants utilising either C_3, C_4, and crassulacean acid metabolism (CAM) pathways for carbon fixation [31,32]. The average $\delta^{13}C$ values obtained from C_3 plant material were between 10 and 15‰ lower compared to the corresponding $\delta^{13}C$ values obtained from C_4 and CAM plant material. Measurement of the isotopic abundance of ^{13}C for lutein isolated from marigold (C_3) and maize (C_4) yielded −29.90±0.20 and −19.77±0.27‰, respectively, showing a similar difference of >10‰ between the two photosynthetic pathways [33].

Although the vast majority of plants belong the C_3 group (>300 000) with bulk $\delta^{13}C$ values of <−24‰, differences in the rate of photosynthesis (mainly caused by differences in climate and geographical location) and in enzyme kinetics of biochemical pathways result in subtle variation of $^{13}C/^{12}C$ ratios that can be detected by GC–C–IRMS. Lockheart et al. were able to detect inter- and intraspecific differences in $\delta^{13}C$ values for *n*-alkanes and alcohols in sun and shade leaves from oak and beech ranging from 0.7 to 3.0‰ [34]. These subtle differences in $\delta^{13}C$ values can be used to determine origin of an organic compound and, thus, the authenticity of a sample.

3.1.1. Authenticity

3.1.1.1. Flavours and fragrances

Bernreuther et al. measured $^{13}C/^{12}C$ isotope ratios of natural and nature-identical γ-decalactone and reported significant differences in $\delta^{13}C$ values that were source dependent although all plants belonged to the C_3 group [35]. For natural γ-decalactone from stone fruit (apricot and peach) they found $\delta^{13}C$ values ranging from −38.0 to −40.8‰, respectively, that were significantly different from $\delta^{13}C$ values of γ-decalactone extracted from soft fruit (strawberry) which were −29.2‰ on average. In contrast, $\delta^{13}C$ values of artificial (nature-identical) γ-decalactone ranged from −24.4 to −26.9‰, whereas γ-decalactone of biotechnological origin showed $\delta^{13}C$ values of −30.8‰ on average.

In an independent study, Mosandl et al. demonstrated the additional advantage to be gained from enantioselective GC–C–IRMS on samples of synthetic γ-decalactone (racemate RAC; 4*R*:4*S*=50:50), γ-decalactone of biotechnological origin (BIO; 4*R*> 99% ee), and a mixture of both (BIO: RAC=60:40) [36]. They reported for the enantiomerically pure (4*R*)-γ-decalactone of biotechnological origin a $\delta^{13}C$ value of −30.12±0.14‰ which is in good agreement with the $\delta^{13}C$ values measured by Bernreuther et al. The separated enantiomers of the nature-identical product showed, as could be expected, identical $\delta^{13}C$ values within the observed standard deviation (4*R*, −28.32±0.36‰; 4*S*, −28.18±0.39‰). Mixing 60% of BIO with 40% of RAC yielded an enantiomeric distribution of 4*R*:4*S*=80:20, with 75% of the 4*R*-configured γ-decalactone being of biotechnological origin. The measured $\delta^{13}C$ value of the 4*R* enantiomer in this mixture was −29.62±0.33‰ which was in good agreement with the theoretically expected value of −29.67‰. The $\delta^{13}C$ value of the 4*S* enantiomer in this mixture was of course the same as for the 4*S* enantiomer in the pure synthetic sample (−28.08±1.30‰).

This early work suggested that two phenomena of biosynthetic pathways, enantioselectivity and mass discrimination (kinetic isotope effects), might serve as compound-specific parameters to establish origin and, hence, to control authenticity of natural flavours and fragrances. However, when focused on indi-

vidual compounds the application of stable isotope abundance measurement is only of limited use as most plants cultivated for human consumption are C_3 plants whose ^{13}C isotopic signatures partially overlap with those of synthetic compounds derived from fossil sources or those of compounds produced by biotechnological methods.

This problem was soon recognised and Mosandl's group suggested the use of genuine internal isotopic standards and formulated the following recommendations [37,38]:

(1) the compound selected as internal isotopic standard should be a genuine characteristic compound of lesser sensorial relevance;

(2) the compound must be available in the sample in sufficient amounts and must not be susceptible to mass discrimination during sample preparation;

(3) the selected compound must be biogenetically related to the compounds under investigation;

(4) chemical inertness of the compound during storage and/or technical processes is mandatory;

(5) the compound selected as internal isotopic standard must not be a legally allowed additive.

The obvious advantage of using an internal standard, biogenetically related to characteristic sample compounds, is the elimination of variations in the $\delta^{13}C$-signature resulting from, e.g., climate-dependent variations of the photosynthetic rate and the kinetic isotope effect associated with the CO_2 fixation step. Therefore, only the characteristic kinetic isotope effects caused by enzymatic reactions during secondary biogenetic pathways are investigated, and the resulting relative $\delta^{13}C$ values can be used as a sample-specific finger print (cf. Fig. 4).

Applying the aforementioned recommendations, Mosandl and co-workers, who have to be regarded as the leaders in the field of authenticity control, studied a wide range of commercially relevant flavours and fragrances and assessed authenticity of allegedly natural samples from commercial sources. The materials studied included lemon oil [37], balm oil [39], citronella oil [39], lemongrass oil [39], coriander oil [40], bergamot oil [41], orange oil [42], mandarin oil [43,44], peppermint oil [45], volatile components from strawberries [16] and apples [46] and α- as well as β-ionone from raspberries [47]. Using self-prepared authentic samples, sample-specific finger prints of six to eight biogenetically related compounds were established based on $\delta^{13}C$ values relative to an internal standard (either limonene, γ-terpinene or neryl acetate). With the help of these finger prints, samples made up entirely of synthetic compounds and even samples containing mixtures of authentic (natural) material and synthetic compounds could be reliably identified. In cases where chiral compounds such as linalol occur naturally as enantiomeric mixtures (in coriander oil, $R{:}S = 20{:}80$), enantioselective GC–C–IRMS could even detect non-authentic samples imitating the natural enantiomeric ratio by measuring the $\delta^{13}C$ values of each enantiomer [40,48].

3.1.1.2. Wine, fruit juice and honey

In the early days of GC–C–IRMS, detection of added sugar in fruit juice and wine was fairly simple as mainly cheap corn syrup (maize: C_4 plant) was predominantly used to boost sugar and/or ethanol content, respectively. Measuring $\delta^{13}C$ values of glucose or bulk carbon was sufficient to prove adulteration. However, addition of small amounts of C_4 plant sugars ($\leq 10\%$) to C_3 plant products such as wine, fruit juice and honey, or the addition of sugars from other C_3 plants (sugar beet; concentrated and deflavourized grape juice) could no longer be detected by these measurements [49]. Schmidt and co-workers studied several methods based on high-precision CSIA to determine authenticity of wine, fruit juices and honey, and to prove fraudulent addition of sugars and even vitamin C from other sources. Their research revealed that in authentic fruit juices biogenetically related compounds such as L-ascorbic acid [50,51], L-malic acid [52] and L-tartaric acid [51] showed $\delta^{13}C$ values strongly correlating with those of their corresponding sugars. For instance, the $\delta^{13}C$ value of L-ascorbic acid is +4.8‰ higher than that of its precursor glucose. This enrichment is mainly located in the C-1 position of L-ascorbic acid of authentic origin and the result of plant-specific kinetic isotope effects during biosynthesis, whereas L-ascorbic acid of biotechnological origin preserves the ^{13}C pattern of glucose [51].

In glycerol originating from natural sources, Weber et al. found a ^{13}C depletion position specific for C-1 and they suggested this unique feature might be used as a means to test for illegal addition of synthetic glycerol to wines [53]. They also discov-

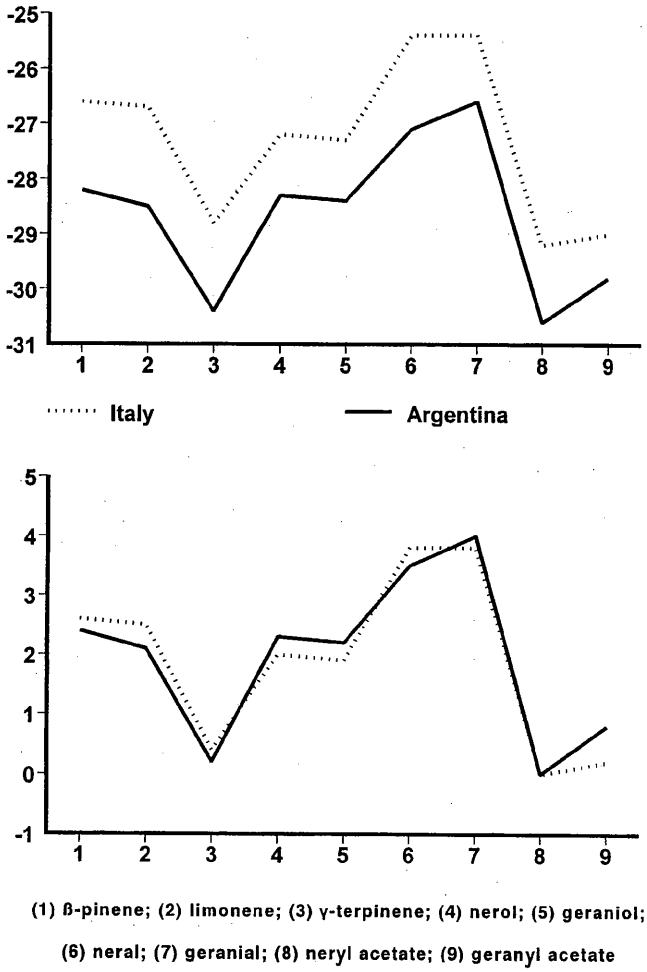

Fig. 4. $\delta^{13}C$ fingerprint of biogenetically related compounds in lemon oils of different geographical origin (top graph). The graph at the bottom shows the $\Delta\delta^{13}C$ fingerprint of the samples obtained when using neryl acetate (8) as internal isotopic standard [38]. From [38], ©Marcel Dekker, 1995.

ered a constant $\Delta\delta^{13}C$ correlation between ethanol and citric acid (+2.4‰) in addition to the known $\Delta\delta^{13}C$ correlation between fermented sugar and ethanol (−1.7‰) [54]. Dennis et al. suggested the use of $\delta^{13}C$ values of sorbitol as a further means for authenticity control of wines [55].

3.1.1.3. *Vegetable oils*

High-quality, single-source vegetable oils are another target for fraudulent adulteration, i.e., partial or total substitution of minor quality and, hence, cheaper oils for the high quality product. In a blind study, Woodbury et al. were able to detect the adulteration of maize germ oil with oils of C_3 plant origin down to a level of 5% (w/w) [56]. They found the saturated 16:0 fatty acid in maize oil to be more depleted in ^{13}C than the corresponding unsaturated fatty acids 18:1 and 18:2. In addition, consistent differences were observed for $\delta^{13}C$ values of vegetable oils from different geographical regions. In a subsequent study, Woodbury et al. determined fatty acid composition and $\delta^{13}C$ values of the major fatty acids of more than 150 vegetable oils [57], thus

establishing a database that provides isotopic information for authenticity control of vegetable oils. Variability in $\delta^{13}C$ values could be related to geographical origin, year of harvest, and the particular variety of oil. Their findings suggest that ultimately $\delta^{13}C$ values of fatty acids are determined by a combination of environmental and genetic factors.

Kelly et al. investigated authenticity of single-seed vegetable oils of C_3 plant origin such as groundnut, palm, rape seed and sunflower oils [58]. They found that the $\delta^{13}C$ values for the authentic vegetable oil fatty acids fell within a narrow range of −27.6 to −32.1‰. Employing canonical discriminant analysis, ^{13}C data from sunflower oil could be separated from other oils, exploiting small, yet significant, differences in $\delta^{13}C$ values within the oil varieties. To detect adulteration of olive oils, Angerosa et al. compared $\delta^{13}C$ values of the aliphatic alcoholic oil fractions and found those of the adulterant pomace oil to be significantly more negative than those of virgin and refined olive oils [59]. Furthermore, they studied isoprenoids and methylsterols isolated from each grade of olive oil and showed the better the olive oil grade, the more positive (i.e., less negative) the $\delta^{13}C$ values of these compounds became.

3.1.1.4. Drugs

Measuring ^{13}C isotopic abundance of heroin to trace the origin of heroin samples in narcotic drug abuse, showed some evidence of variation in $\delta^{13}C$ values of heroin depending on its geographical site of production [60]. A preliminary study to trace the origin of different batches of confiscated 3,4-(methyldioxy)methylamphetamine (MDMA, Ecstasy) tablets by GC–C–IRMS allowed the discrimination of four different groups of MDMA tablets based on variations in their NA $\delta^{13}C$ values [61]. The same study showed that further discrimination could be obtained when using $\delta^{15}N$ values of MDMA.

Prompted by the uncertainty associated with the T/E>6 test that measures the ratio of testosterone (T) and epitestosterone (E) and the high public interest in alleged doping in athletes, several studies have been carried out to use metabolic pathway related ^{13}C isotope patterns to differentiate between endogenous human testosterone and exogenous testosterone [62]. In the human body, testosterone is synthesised from cholesterol via dehydroepiandrosterone and is then further metabolised to androstanediol. The group around Aguilera et al. found that the averaged $\delta^{13}C$ values for endogenous 5α- and 5β-androstanediol dropped from −26.52‰ before synthetic testosterone administration (natural background or baseline value) to −32.44‰ during testosterone administration [63]. Independent work by Shackleton et al. obtained a similar baseline $\delta^{13}C$ value of −26.87‰ and a drop down to −30.21‰ on average for androstanediol samples after a bolus administration of 250 mg exogenous testosterone [64,65]. This drop of about −2‰ lasted for up to 10 days before $\delta^{13}C$ values of androstanediol returned to their former baseline value. They also reported a narrow range of −29.15 to −30.41‰ for five synthetic testosterone samples manufactured in five different countries. Based on the results reported by Aguilera et al. [63] and their own, Shackleton et al. suggested a conservative cut-off value of −29.0‰ for androstanediol to identify unambiguously testosterone abuse for up to 7 days after administration.

Hydrocortisone abuse in horse racing and other equine sports can be confirmed on the basis of significantly different ^{13}C isotope patterns between endogenous urinary hydrocortisone and synthetic material. This method, proposed by Aguilera et al., employs conversion of urinary hydrocortisone into its bismethylenedioxy derivative to improve its gas chromatographic properties [66].

3.1.2. Origin

3.1.2.1. Geochemistry

The desire to study ^{13}C isotope abundance of sedimentary hydrocarbons on a molecular level was one of the driving forces behind the development of GC–C–IRMS. Geochemists and archaeologists wanted to extract all possible information contained in fossil biomarkers such as sedimentary long-chain alcohols and sterols [67], triterpene-derived hydrocarbons [68], neutral monosaccharides [69], long-chain alkanes [70–74], alkanes and isoprenoids [75,76], polycyclic aromatic hydrocarbons (PAHs) [77], amino acids [78–80] and phenolic acids [81].

Freeman et al. measured hydrocarbons from sediments deposited in the Messel shale and found a wide spectrum of $\delta^{13}C$ values ranging from −20

down to −75‰, thus proving the equally wide spectrum of origins [82]. The extreme negative values were thought to indicate the activity of methanotrophic bacteria, as $\delta^{13}C$ values of < -45‰ thus far had only been observed for methane but not for larger molecules. This and others studies [68,69,73,83] demonstrated that sedimentary organic compounds contain contributions of bacterial origin rather than being solely of plant origin. Using GC–C–IRMS to measure ^{13}C isotope abundance in hydrocarbons from sedimentary rocks across the Precambrian–Cambrian boundary, Logan et al. [84] were able to shed some light on the development of multicellular life during the so-called 'Cambrian explosion'. Based on the isotopic data, they could show a transition from an environment dominated by sulphate-reducing bacteria to one dominated by photosynthetic organisms, thus transforming the hitherto anaerobic ocean into an aerobic ocean.

3.1.2.2. Archaeology

Measuring $^{13}C/^{12}C$ isotope ratios has become an increasingly important tool to glean information on prehistoric diet and lifestyle from organic residues preserved in archaeological artefacts. Employing both HTcGC–MS and HTcGC–C–IRMS to identify chemical structures and measure $\delta^{13}C$ values, respectively, Evershed et al. showed that lipid extracts (C_{25}–C_{33} alkanes and a C_{29} ketone, nonacosain-15-one) from organic residues found in archaeological potsheds were derived from *Brassica* species (wild-type cabbage) [85]. Later work on organic residues from archaeological pottery vessels found C_{31}, C_{33} and C_{35} ketones with $\delta^{13}C$ values that were up to 10‰ higher than those found for the C_{29} ketones from wild-type *Brassica* species. Based on HTcGC–MS and HTcGC–C–IRMS data, Evershed and co-workers formed the hypothesis that a precursor/product relationship may exist between C_{35} ketones and fatty acids, and corresponding triacylglycerols such as tripalmitin and tristearin from animal fats [86]. Studying pyrolysis reactions of acyl lipids and monitoring their products by HTcGC–MS and HTcGC–C–IRMS, they could confirm that C_{31}, C_{33} and C_{35} mid-chain ketones found in archaeological pottery vessels were indeed derived from a mixture of free fatty acids [87]. Comparing carbon number distributions of triacylglycerols and $\delta^{13}C$ values of 16:0 and 18:0 acyl moieties of lipid compounds from extracts of neolithic vessels with modern reference animal fats, Evershed et al. could identify animal fat residues found in vessels dated circa 4200 BP as being close to reference pig adipose fats, whereas residues found in vessels dated circa 4500 BP were closer to reference ruminant fat [88].

O'Donoghue et al. reported $\delta^{13}C$ values in the range of −25.4 to −29.2‰ for the principal fatty acids (16:0 to 24:1) of radish seed found in a 6th century AD storage vessel [89]. Composition and $\delta^{13}C$ values of fatty acids found in the ancient radish seeds matched closely those found in modern radish seeds.

Stott et al. measured $\delta^{13}C$ values of cholesterol and 3β-hydroxycholest-5-en-7-one from fossil whale bones [90] and archaeological human bones and teeth [91], and showed that their ^{13}C content could be used as an important new source of palaeodietary information. Another insight into prehistoric life was gleaned from the ^{13}C analysis of adsorbed lipids preserved in the fabric of Minoan lamps and conical cups. The $\delta^{13}C$ values together with HTcGC–MS profiles identified beeswax as the illuminant burned in prehistoric Aegean lamps rather than olive oil as hitherto supposed [92].

3.1.2.3. Environmental chemistry

Monitoring environmental and climate changes by measuring $\delta^{13}C$ values of atmospheric gases such as methane, carbon monoxide and carbon dioxide has traditionally been carried out using dual-inlet IRMS systems. Their measurements however, required time-consuming sample preparation of large sample volumes. The high abundance sensitivity of GC–C–IRMS together with the use of PLOT fused-silica capillary columns for routine GC analysis of highly volatile organic compounds (HVOCs) has now become the method of choice for scientists as air samples between 50 μl and 5 ml can be analysed on-line without any prior sample preparation [93–95].

High-precision CSIA by GC–C–IRMS is also used to determine origin and identify sources of oil spills and oil pollution [96–98], ocean-transported bitumen [99], characterisation of refractory wastes at heavy-oil contaminated sites [100,101] and to trace

the sources of PAHs in the environment [102–104]. Bird et al. used GC–C–IRMS to record the $\delta^{13}C$ values of individual biomarker compounds (*n*-alkanes) to assess vegetation changes [105], whereas Naraoka et al. measured differences in $\delta^{13}C$ values of long-chain fatty acids (C_{20}–C_{30}) that had been extracted from terrestrial and marine sediment [106].

3.2. Tracer studies

The high abundance sensitivity of GC–C–IRMS has also been increasingly exploited in metabolic studies investigating turnover, incorporation and synthesis processes in vivo that could previously only be investigated either with stable isotope tracers at high enrichment level using GC–MS, or not at all. The latter usually for reasons of excessive tracer dilution in the various metabolic pools and/or low incorporation rates. Although in these cases radioactive tracers can provide an alternative, their use is associated with certain risks which are nowadays regarded as unacceptable especially when dealing with members of the paediatric age group.

GC–C–IRMS proved to be a decisive tool in determining if and to what extent neonates and premature infants of very low birth weight could synthesise arachidonic acid, which is essential for their growing tissues, from dietary fatty acids. Demmelmair et al. could show that in neonates fed on a phenylalanine-free diet, on average 23% of free plasma arachidonic acid on study day 4 originated from infantile linoleic acid conversion [107]. They determined ^{13}C content of linoleic acid and arachidonic acid in 0.25–0.5 ml serum before and for 4 days after the infants' diet contained corn oil. Baseline $\delta^{13}C$ values for linoleic acid and arachidonic acid were -31.5 ± 1.1 and -30.1 ± 1.2‰, respectively; after 4 days, changes in $\delta^{13}C$ values over baseline were $+12.7\pm0.7$ and $+2.7\pm0.7$‰, respectively. Carnielli et al. added linoleic acid and linolenic acid, both ^{13}C-labelled, to the formula diet which was administered continuously for 48 h (birth weight, 1.17 ± 0.12 kg; gestational age, 28.4 ± 1.3 weeks) [108]. They could show that both tracers were rapidly incorporated into plasma phospholipids and that their metabolic products including arachidonic acid and docosahexaenoic acid became highly enriched with ^{13}C. Incorporation of ^{13}C-octanoic acid into plasma triglycerides (10% of the enrichment of the diet), noticeably into myristic and palmitic acid, by very low-weight preterm infants was reported earlier by the same group [109].

A similar observation was made during a study with an entirely different objective. Using GC–C–IRMS, Koziet et al. could demonstrate that ethanol itself may be used as a substrate for lipogenesis, although only to a small extent [110]. They calculated that $<10\%$ of fatty acids contained in very-low-density lipoproteins (VLDL) triglycerides were derived from this pathway, with ethanol predominantly being incorporated into myristic and palmitic acid.

The majority of ^{13}C tracer studies published have dealt with various aspects of fatty acid biochemistry, such as metabolism of triglycerides [111,112], and transport and turnover of free saturated [113–115] and unsaturated fatty acids [116–120]. While studying the metabolism of ^{13}C-labelled polyunsaturated fatty acids by ^{13}C NMR, using GC–C–IRMS, Cunnane et al. found low levels of ^{13}C-labelled γ-linolenic acid in brain phospholipids of suckling rat pups that could not be detected by ^{13}C NMR [121].

Employing ^{13}C tracers at low levels of enrichment, reliable data were obtained in studies of the kinetics of glucose [122,123] and glycoprotein neutral sugars [124,125], cholesterol and lipoproteins [126], phosphatidylcholine [127], urea [128,129], branched-chain amino acid metabolism [130], measuring protein fractional synthetic rates [131] and protein synthesis in colorectal cancer cells [132,133]. Roscher et al. used L-rhamnose with two different levels of ^{13}C abundance in parallel experiments to determine if L-rhamnose serves as a carbon source for furaneol [134].

Unlike GC–MS, where increasing the amount of label has no general effect on detection limits, in GC–C–IRMS, increasing label enrichment in precursor compounds produces significantly improved detection limits. In a recent review of high-precision CF–IRMS, Brenna et al. discussed theoretical and practical considerations for this type of study [135]. High-precision CSIA in this type of tracer studies has been shown to possess advantages over organic GC–MS for stable isotopic tracer detection and to be